International Journal of Modern Physics E
© World Scientific Publishing Company

FISSION BARRIERS OF SUPERHEAVY NUCLEI IN THE SKYRME-HARTREE-FOCK MODEL

ANDRZEJ STASZCZAK

Institute of Physics, Maria Curie-Skłodowska University
pl. M. Curie-Skłodowskiej 1, 20-031 Lublin, Poland
stas@tytan.umcs.lublin.pl

JACEK DOBACZEWSKI

Institute of Theoretical Physics, Warsaw University, ul. Hoża 69, 00-681 Warsaw, Poland
jacek.dobaczewski@fuw.edu.pl

WITOLD NAZAREWICZ

Department of Physics and Astronomy, University of Tennessee Knoxville, TN 37996, USA
Physics Division, Oak Ridge National Laboratory P.O. Box 2008, Oak Ridge, TN 37831, USA
Institute of Theoretical Physics, Warsaw University ul. Hoża 69, 00-681 Warsaw, Poland
witek@utk.edu

Received (received date)
Revised (revised date)

Constrained Skyrme-Hartree-Fock calculations of static fission barriers are performed for even-even elements with $Z = 100 \div 110$ as well as for superheavy N=184 isotones. In our study we use the Skyrme parametrization SLy4 and a seniority pairing force treated in the BCS approximation. The computations are carried out applying a code that makes it possible to break all self-consistent symmetries of the nuclear mean field, including axial symmetry and reflection symmetry. The influence of reflection-asymmetric and triaxial degrees of freedom on fission barriers are discussed.

1. Introduction

Spontaneous fission plays a significant role in a disintegration process of the superheavy elements (SHE). Microscopically, this phenomenon can be viewed as a many-body tunneling through a potential barrier. Studies of fission barriers are important for the determination of the stability of the heaviest nuclei.

Recently, a number of theoretical calculations of fission barriers of SHE have been carried out. These include calculations based on the microscopic-macroscopic treatment[1,2], the self-consistent approach with the Gogny[3] and Skyrme[4,5,6,7] forces, and also within the relativistic mean-field model[5,8,9].

The objective of this contribution is to study static fission barriers of the even-even SHE in the Skyrme-Hartree-Fock (SHF) approach with a seniority pairing force treated in the BCS approximation. We focus on two regions of SHE: (i) the

deformed nuclei with $100 \leq Z \leq 110$, and (ii) spherical isotones with N=184.

The calculations have been carried out using the code HFODD (v.2.09i)[10,11,12] that solves self-consistent HF equations by using the Cartesian harmonic oscillator (HO) finite basis. This code makes it possible to break all self-consistent symmetries of the nuclear mean field at the same time, including the axial and reflection symmetry, which is of particular interest in the present study.

Particular attention has been paid to symmetry-breaking effects along the fission path. The influence of reflection-asymmetric (for a non-zero octupole mass moment, $Q_{30} \equiv \langle \hat{Q}_{30} \rangle \neq 0$) and triaxial degrees of freedom (for $Q_{22} \neq 0$) on the static fission barriers are discussed.

2. Fission barriers in the SHF+BCS model

In our SHF+BCS model, we have used the energy density functional with the Skyrme interaction SLy4[13] and the pairing force strengths defined as in Ref.[14]. Additionally, for the deformed SHE with $100 \leq Z \leq 110$, the pairing strengths have been scaled to reproduce the experimental[15] neutron (0.696 MeV) and proton (0.803 MeV) pairing gaps in ^{252}Fm. For the superheavy isotones with N=184, whose experimental nuclear masses are unknown, the pairing strengths have been scaled to reproduce the pairing gaps of the finite-range droplet model (FRDM)[16].

For all nuclei considered, a self-consistent total binding energy ($E^{\rm tot}$) is computed with a quadratic constraint[17] on the mass quadrupole moment Q_{20}. Our study covers the prolate deformations $Q_{20} = 0 \div 300\,$b (barns) with a step of 10 b for prolate deformed SHE and the oblate/prolate deformations $Q_{20} = -30 \div 300\,$b in the case of spherical SHE. To fix the position of the nucleus center of mass, an additional constraint on the mass dipole moment, $Q_{10} = 0$, is assumed.

2.1. *Fission barriers for deformed SHE with* $100 \leq Z \leq 110$

The nuclei from this region are well deformed in their ground states. It is worth noting that their stability is determined by the deformed subshell closures at neutron numbers N=152 for the isotopes of fermium (Z=100) and nobelium (Z=102), and N=162 for the isotopes of hassium (Z=108).

Figures 1 and 2 show the total binding energies ($E^{\rm tot}$) and mass octupole moments (Q_{30}) calculated for the even-even fermium and nobelium isotopes, respectively, as functions of the mass quadrupole moment Q_{20}. The predicted static barriers have a two-humped shape with an inner barrier greater than an outer one. The sizes of fission barriers are well correlated with the 'magic' deformed neutron number N=152. Indeed, one can see that the barriers reach their local maxima for ^{252}Fm and ^{254}No. For the heavier isotopes with N>152, the second barriers collapse and practically disappear for N=162 (in Fm isotopes) and for N=160 (in No isotopes).

The disappearance of the second barrier is related to the transition from the reflection-symmetric ($Q_{30} = 0$) fission path to the reflection-asymmetric fission

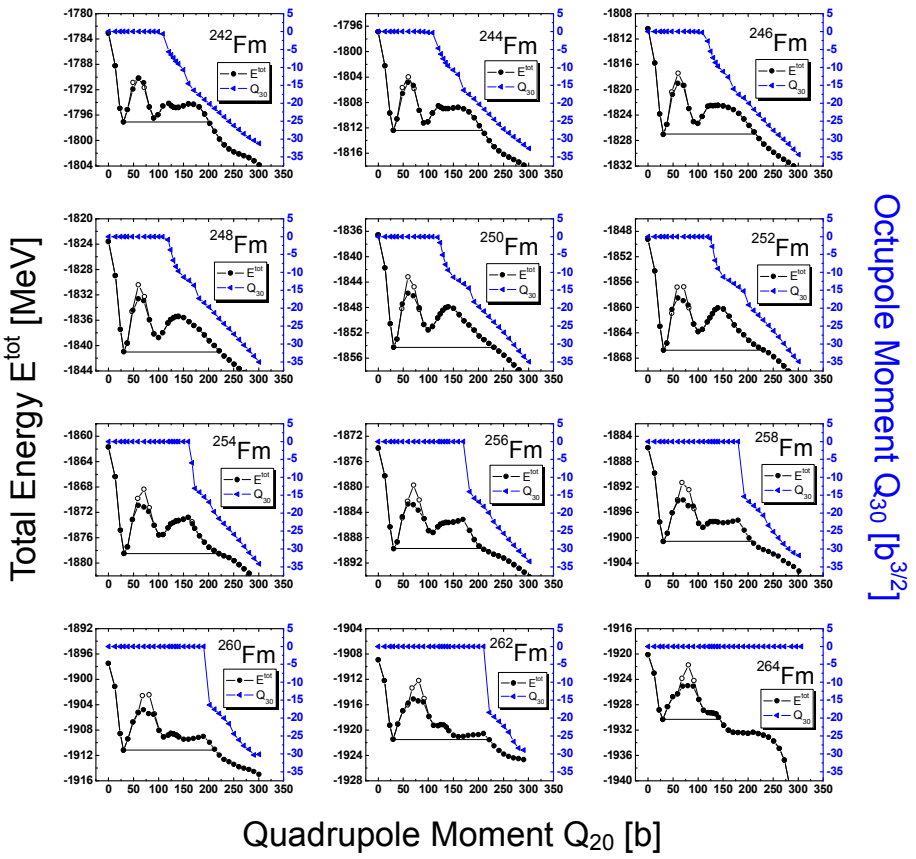

Fig. 1. The total binding energies $E^{\rm tot}$ (●, scales on the left-hand sides) and the mass octupole moments Q_{30} (◀, scales on the right-hand sides) calculated along the lowest static fission paths for the even-even fermium isotopes. The differences between the open and solid symbols in the region of the first barrier represent the energy reduction due to the presence of triaxial distortions.

path ($Q_{30} \neq 0$). For the heavier Fm and No isotopes, a switch from the reflection-symmetric to the reflection-asymmetric nuclear shapes occurs at greater values of Q_{20}. In the extreme cases of ^{264}Fm (when a fission into the two doubly magic ^{132}Sn nuclei is expected) and ^{264}No, the static fission paths appear to be reflection-symmetric. The reduction of the second barrier plays a crucial role in the standard interpretation of the experimentally known rapid decrease of the spontaneous fission half-lives in the heavy Fm and No isotopes.

The influence of triaxiality ($Q_{22} \neq 0$) on the first fission barrier is given by the difference between the open and solid symbols in Figs. 1 and 2. The effect of triaxiality increases with the neutron number, reaching a peak value of about 3 MeV.

The total binding energies ($E^{\rm tot}$) and mass hexadecapole moments (Q_{40}) cal-

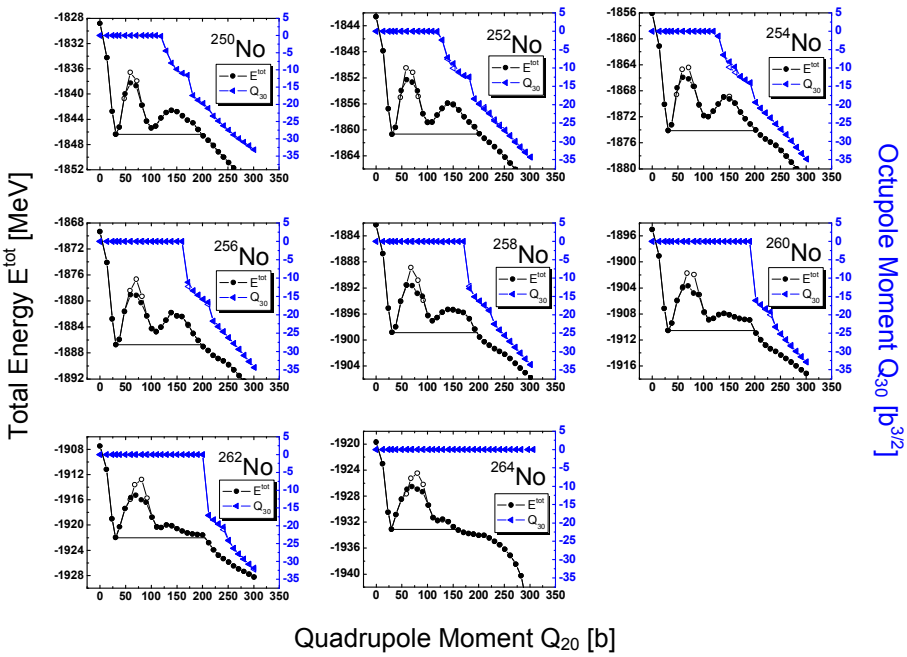

Fig. 2. Similar as in Fig. 1 except for the even-even nobelium isotopes.

culated along the static fission paths in the even-even rutherfordium (Z=104), seaborgium (Z=106), hassium (Z=108), and darmstadtium (Z=110) isotopes are shown in Figs. 3 and 4. We have found that almost all of these nuclei have purely reflection-symmetric static fission paths. Only in the case of ^{254}Rf, ^{256}Rf, and ^{258}Sg have the reflection-asymmetric paths been observed (results not shown). One can see that the hexadecapole moments gradually increase along the paths to fission. It is worth noting that a similar behavior of Q_{40} has been also observed for Fm and No isotopes. The reduction of fission barriers in Figs. 3 and 4 due to triaxiality is similar to that calculated for Z=100 and 102.

With the increase of proton number from Z=100 to 110, one can notice two effects, namely, (i) the disappearance of the outer barriers, and (ii) the decrease of the inner barriers. The first of these effects can be seen in Figs. 3B and 4 which display one-humped, narrow barriers predicted for Sg, Hs, and Ds. The second effect is particularly evident for the heaviest ^{276,278}Ds isotopes having barriers reduced by a factor of two as compared to ^{252}Fm.

2.2. *Fission barriers for the spherical N=184 isotones*

Figure 5 shows the total binding energies and mass hexadecapole moments (Q_{40}) calculated for twelve even-even N=184 isotones as a function of the mass quadrupole moment Q_{20}. One can see that the N=184 systems are all spherical in their

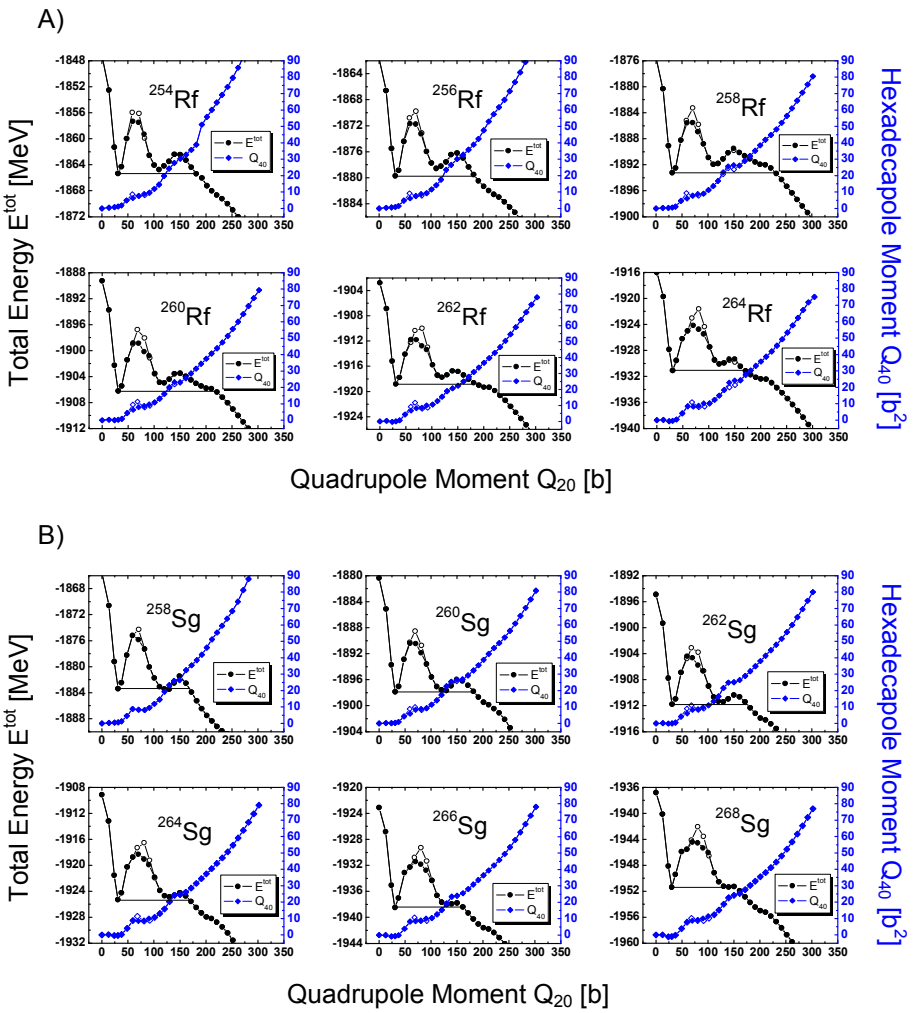

Fig. 3. The total binding energies $E^{\rm tot}$ (●, scales on the left-hand sides) and the mass hexadecapole moment Q_{40} (⧫, scales on the right-hand sides) as functions of Q_{20} for the even-even isotopes of rutherfordium (**A**) and seaborgium (**B**). The differences between the open and solid symbols represent the effects of triaxiality on the first barrier.

ground states (cf. Ref.[18] and references quoted therein). It has also been found that all of these SHE have reflection-symmetric static fission paths. Similarly, as for the deformed heavy nuclei discussed above, the mass hexadecapole moments along the fission path continually increase their values from 0 up to 80 b^2.

The reduction of fission barriers due to the appearance of triaxial deformations, seen in Fig. 5 as the difference between the open and solid symbols, strongly depends on proton number. The largest effect has been predicted for the nucleus $^{310}126_{184}$ where the barrier reduction exceeds 3 MeV. However, in the case of the isotones

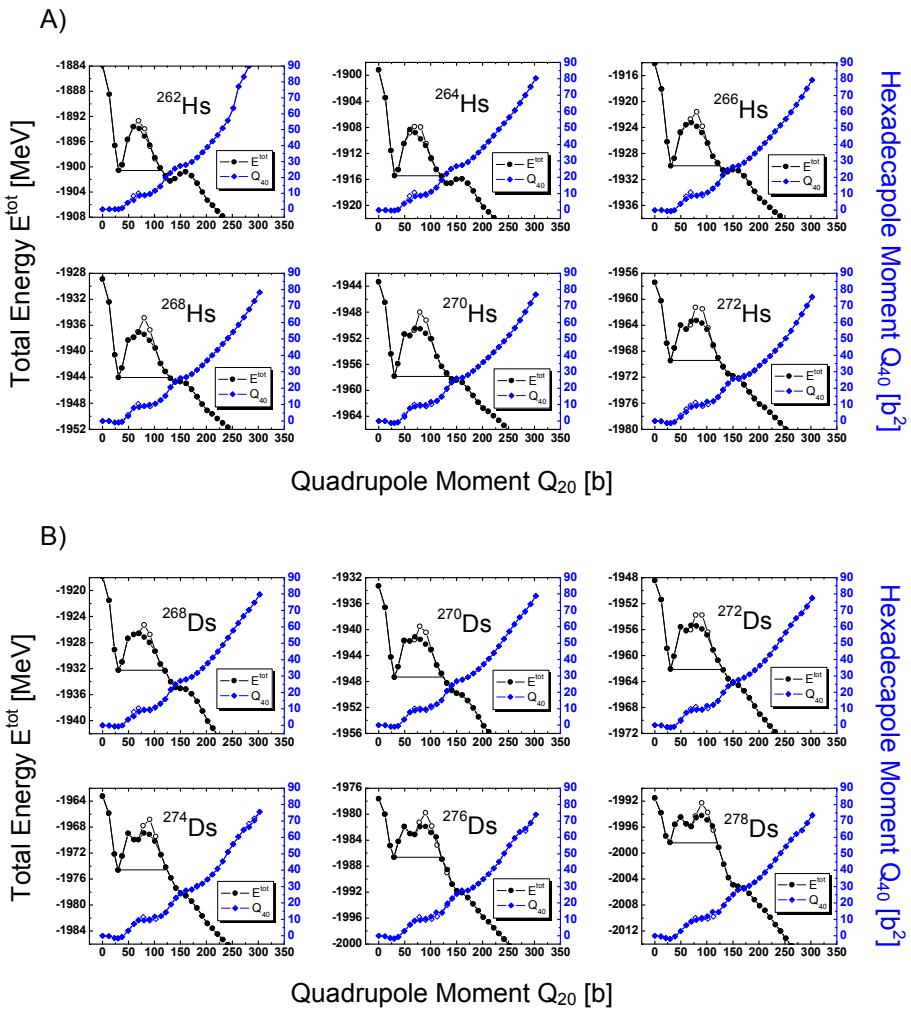

Fig. 4. Similar as in Fig. 3 except for the even-even hassium (**A**) and darmstadtium (**B**) isotopes.

with $Z \leq 114$, triaxiality plays a minor role.

Studying static fission barriers can offer useful insights concerning the stability of SHE. Comparison of the sizes of static fission barriers in the $N=$ 184 isotones shown in Fig. 5 hints at a possible increased stability against spontaneous fission for $^{302}118_{184}$ and $^{304}120_{184}$.

The neutron (▲) and proton (▼) pairing gaps calculated along the static fission paths for SHE with N=184 are shown in Fig. 6. The solid (open) symbols represent results obtained with (without) triaxial deformations. The values of pairing gaps in the spherical ground states correspond to the FRDM estimates[16]. As one can see, for all the SHE presented in Fig. 6, the average value of Δ_n fluctuates between 1

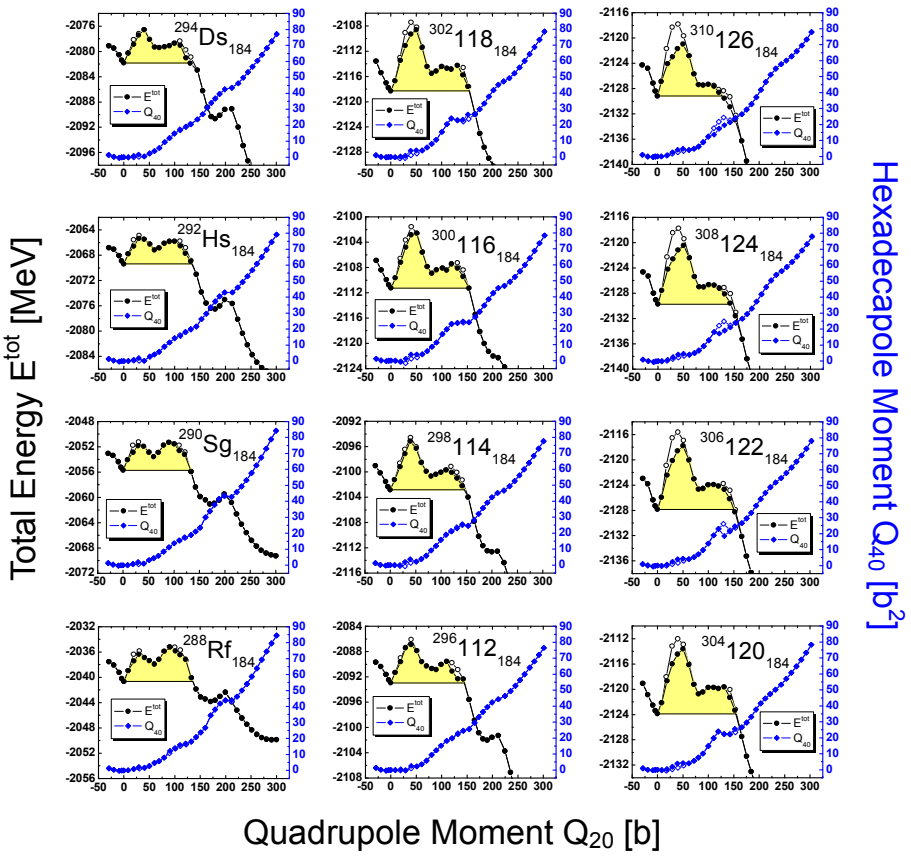

Fig. 5. Similar as in Fig. 3 except for the even-even isotones with N=184.

and 1.5 MeV. On the other hand, the average Δ_p for all the isotones up to $^{304}120_{184}$ is around 0.5 MeV. For the heaviest nuclei with Z= 122, 124, and 126, Δ_p steadily increases reaching the value of Δ_n for $^{310}126_{184}$. These results, obtained within the seniority pairing approximation, do not take into account the fact that structure of the single-particle orbitals may change along the fission paths. Such effects can be included by calculating pairing matrix elements from a zero-range pairing force, which will be the subject of a future analysis.

3. Conclusion

The Skyrme energy density functional with the SLy4 parametrization has been applied to study static fission barriers of even-even SHE with $100 \leq Z \leq 110$ and even-even spherical isotones with N= 184. Our calculations take into account axial- and reflection-symmetry-breaking effects along the static fission paths.

For all the nuclei investigated, the appearance of triaxial deformations reduces

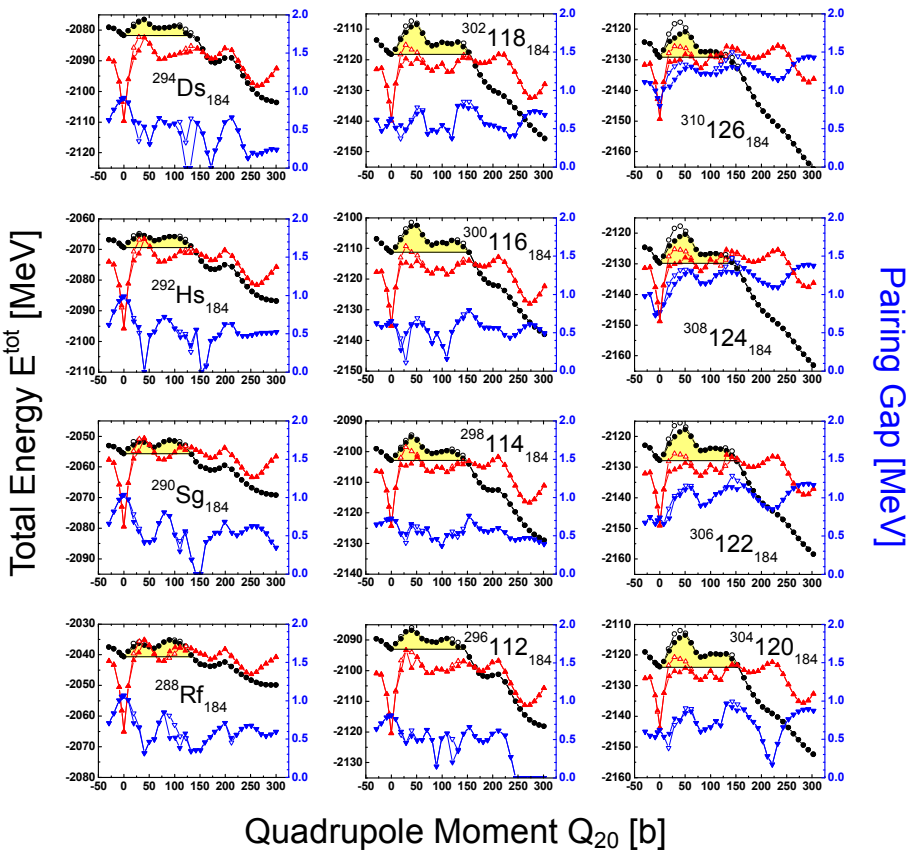

Fig. 6. The total binding energies $E^{\rm tot}$ (●, scales on the left-hand sides) and the neutron (▲) and proton (▼) pairing gaps (scales on the right-hand sides) for the N=184 isotones shown in Fig. 5. The differences between open and solid symbols illustrate the effects of triaxiality.

the inner barrier by up to 3 MeV. It has also been found that the strongest reflection-symmetry-breaking effects appear in ^{258}Sg, ^{254,256}Rf, and in the Fm and No isotopes (excluding ^{264}Fm and ^{264}No). In all remaining cases, purely reflection-symmetric fission paths have been predicted. The analysis of the static fission barriers of even-even nuclei with N=184 hints at an increased stability against spontaneous fission for Z= 118 and 120.

Acknowledgements

This work was supported in part by the National Nuclear Security Administration under the Stewardship Science Academic Alliances program through the U.S. Department of Energy Research Grant DE-FG03-03NA00083; by the U.S. Department of Energy under Contract Nos. DE-FG02-96ER40963 (University of Tennessee) and DE-AC05-00OR22725 with UT-Battelle, LLC (Oak Ridge National

Laboratory); by the Polish Committee for Scientific Research (KBN) under Contract No. 1 P03B 059 27; and by the Foundation for Polish Science (FNP).

References

1. A. Baran, Z. Łojewski, and K. Sieja, *Int. J. Mod. Phys.* **E 13**, 353–356 (2004).
2. A. Baran, Z. Łojewski, K. Sieja, and M. Kowal, *Phys. Rev. C* **72** (2005) - in print.
3. M. Warda, J. L. Egido, L. M. Robledo, and K. Pomorski, *Phys. Rev. C* **66**, 014310 (2002).
4. L. Bonneau, P. Quentin, and D. Samsœn, *Eur. Phys. J.* **A 21**, 391–406 (2004).
5. T. Bürvenich, M. Bender, J. A. Maruhn, and P.-G. Reinhard, *Phys. Rev. C* **69**, 014307 (2004).
6. A. Staszczak, J. Dobaczewski, and W. Nazarewicz, *Int. J. Mod. Phys.* **E 14**, 395–402 (2005).
7. A. Staszczak, J. Dobaczewski, and W. Nazarewicz, *Proc. 3rd International Workshop on Nuclear Fission and Fission-Product Spectroscopy, Cadarache, 2005* (AIP Conference Proceedings) - in print.
8. W. Zhang, J. Meng, S. Q. Zhang, L. S. Geng, and H. Toki, *Nucl. Phys.* **A753**, 106–135 (2005).
9. T. Sil, S.K. Patra, B.K. Sharma, M. Centelles, and X. Viñas, *Phys. Rev. C* **69**, 044315 (2005).
10. J. Dobaczewski and J. Dudek, *Comput. Phys. Commun.* **102**, 166–182 (1997); *ibid.* **102**, 183–209 (1997); *ibid.* **131**, 164–186 (2000).
11. J. Dobaczewski and P. Olbratowski, *Comput. Phys. Commun.* **158**, 158–191 (2004); *ibid.* **167**, 214–216 (2005).
12. http://www.fuw.edu.pl/∼dobaczew/hfodd/hfodd.html
13. E. Chabanat, P. Bonche, P. Haensel, J. Meyer, and F. Schaeffer, *Nucl. Phys.* **A635**, 231 (1998); **A643**, 441(E) (1998).
14. J. Dudek, A. Majhofer, and J. Skalski, *J. Phys.* **G6**, 447 (1980).
15. G. Audi, A. H. Wapstra, and C. Thibault, *Nucl. Phys.* **A729**, 337–676 (2003); http://csnwww.in2p3.fr/amdc/masstables/Ame2003/rct7.mas03
16. P. Möller, J. R. Nix, and K.-L. Kratz, *At. Data Nucl. Data Tables* **66**, 131–343 (1997); http://t2.lanl.gov/data/astro/molnix96/pairlip.dat
17. H. Flocard, P.Quentin, A. K. Kerman, and D. Vautherin, *Nucl. Phys.* **A203**, 433–472 (1973).
18. S. Ćwiok, P. H. Heenen, and W. Nazarewicz, *Nature* **433**, 705–709 (2005).